

Measurements of the CKM Angle α at BaBar

S. Stracka on behalf of the BaBar Collaboration

Università degli Studi di Milano and INFN, Sezione di Milano - I-20133 Milano, Italy

We present improved measurements of the branching fractions and CP -asymmetries in the $B^0 \rightarrow \pi^+\pi^-$, $B^0 \rightarrow \pi^0\pi^0$, and $B^+ \rightarrow \rho^+\rho^0$ decays, which impact the determination of α . We find

$$\begin{aligned} S_{\pi\pi}^{+-} &= -0.68 \pm 0.10 \pm 0.03 \\ C_{\pi\pi}^{+-} &= -0.25 \pm 0.08 \pm 0.02 \\ C_{\pi\pi}^{00} &= -0.43 \pm 0.26 \pm 0.05 \\ \mathcal{B}(B^0 \rightarrow \pi^0\pi^0) &= (1.83 \pm 0.21 \pm 0.13) \times 10^{-6} \end{aligned}$$

for $B \rightarrow \pi\pi$ decays, and

$$\begin{aligned} \mathcal{B}(B^+ \rightarrow \rho^+\rho^0) &= (23.7 \pm 1.4 \pm 1.4) \times 10^{-6} \\ f_L(\rho^+\rho^0) &= 0.950 \pm 0.015 \pm 0.006 \\ \alpha_{\rho\rho} &= (92.4_{-6.5}^{+6.0})^\circ \end{aligned}$$

for $B \rightarrow \rho\rho$ decays.

The combined branching fractions of $B \rightarrow K_1(1270)\pi$ and $B \rightarrow K_1(1400)\pi$ decays are measured for the first time and allow a novel determination of α in the $B^0 \rightarrow a_1(1260)^\pm\pi^\mp$ decay channel. We obtain

$$\begin{aligned} \mathcal{B}(B^0 \rightarrow K_1(1270)^+\pi^- + K_1(1400)^+\pi^-) &= (3.1_{-0.7}^{+0.8}) \times 10^{-5} \\ \mathcal{B}(B^+ \rightarrow K_1(1270)^0\pi^+ + K_1(1400)^0\pi^+) &= (2.8_{-1.7}^{+2.9}) \times 10^{-5} \\ \alpha_{a_1\pi} &= (79 \pm 7 \pm 11)^\circ. \end{aligned}$$

These measurements are performed using the final dataset collected by the BaBar detector at the PEP-II B-factory.

1. Introduction

The primary goal of the experiments based at the B factories is to test the Cabibbo-Kobayashi-Maskawa (CKM) picture of CP violation in the standard model of electroweak interactions [1]. This can be achieved by measuring the angles and sides of the Unitarity Triangle in a redundant way.

An effective value α_{eff} for the CKM phase $\alpha \equiv \arg(-V_{td}V_{tb}^*/V_{ud}V_{ub}^*)$ can be extracted from the time-dependent analysis of B meson decays dominated by tree-level $b \rightarrow u\bar{u}d$ amplitudes, such as $B^0 \rightarrow \pi^+\pi^-$, $B^0 \rightarrow \rho^+\rho^-$, $B^0 \rightarrow \rho^\pm\pi^\mp$, and $B^0 \rightarrow a_1(1260)^\pm\pi^\mp$. The current average values of α , $\alpha = (92 \pm 7)^\circ$ [2] and $\alpha = (89_{-4.2}^{+4.4})^\circ$ [3], obtained with different statistical techniques, are based solely on the analysis of $B \rightarrow \pi\pi$, $B \rightarrow \rho\rho$, and $B \rightarrow \rho\pi$ decays.

The measurement of the angle α has witnessed significant progress over the past year. The following sections are organized as follows: a brief introduction on the experimental technique is given in Sec. 2; the summer 2008 update of the measurement of the time-dependent CP -violating asymmetries in $B^0 \rightarrow \pi^+\pi^-$ decays and of the branching fractions (BFs) of $B^0 \rightarrow \pi^0\pi^0$ decays is reported in Sec. 3; Sec. 4 describes the 2009 update of the BF measurement of $B^+ \rightarrow \rho^+\rho^0$ decays, and its impact on the precision of the determination of α ; in Sec. 5, we introduce the first measurement of $B \rightarrow K_1(1270)\pi$ and $B \rightarrow K_1(1400)\pi$ decays and a new determination of α

in $B^0 \rightarrow a_1(1260)^\pm\pi^\mp$ decays.

2. Experimental techniques

The interference between the direct tree decay (which carries the weak phase γ) and decay after $B^0\bar{B}^0$ mixing (which carries a weak phase 2β) results in a time-dependent decay-rate asymmetry that is sensitive to the angle $2\beta + 2\gamma = 2\pi - 2\alpha$.

At the asymmetric-energy e^+e^- B-factory PEP-II, running at a center of momentum (CM) energy of 10.58 GeV, a $B\bar{B}$ pair is coherently produced in the decay of a $\Upsilon(4S)$ resonance. The resulting $B\bar{B}$ system has a boost $\beta\gamma \approx 0.56$ with respect to the laboratory frame. By means of this experimental device it is possible to measure the decay vertex displacement Δz of the two B mesons in the event, and hence their proper-time difference $\Delta t_{\text{meas}} \approx \frac{\Delta z}{\beta\gamma c}$.

One of the B mesons (B_{rec}) is fully reconstructed according to the final state of interest. In order to study the time-dependence of the decay rates, it is necessary to measure the proper-time difference Δt between the two B mesons in the event and to identify the flavor of the other B -meson (B_{tag}). The flavor and the decay vertex position of B_{tag} are therefore identified from its decay products.

The decay-rate distribution for B^0 (\bar{B}^0) decays to

a CP -eigenstate, such as $\pi^+\pi^-$, is given by:

$$\frac{dN}{d\Delta t} = \frac{e^{-|\Delta t|/\tau}}{4\tau} \left\{ 1 - q_{tag} \left[C \cos(\Delta m_d \Delta t) - S \sin(\Delta m_d \Delta t) \right] \right\}, \quad (1)$$

where $\tau = (1.536 \pm 0.014)$ ps [4] is the mean B lifetime, $\Delta m_d = (0.502 \pm 0.007)$ ps $^{-1}$ is the $B^0 - \bar{B}^0$ mixing frequency [4], and $q_{tag} = +1$ (-1) if the B_{tag} decays as a B^0 (\bar{B}^0). The parameters S and C describe mixing-induced and direct CP -violation, respectively, and are defined as:

$$S = \frac{2\text{Im}\lambda}{1 + |\lambda|^2}, \quad C = \frac{1 - |\lambda|^2}{1 + |\lambda|^2},$$

with $\lambda = \frac{q}{p} \frac{\bar{A}}{A}$, where q/p is related to the $B^0 - \bar{B}^0$ mixing, and A (\bar{A}) is the amplitude of the decay of a B^0 (\bar{B}^0) to the final state under study. If only the tree amplitude contributes to the decay, $S = \sin(2\alpha)$ and $C = 0$. However, $b \rightarrow u\bar{u}d$ transitions receive sizeable contributions from penguin (loop) amplitudes, which carry different strong and weak phases. This contribution can result in non-zero direct CP -violation $C \neq 0$ and modifies S into

$$S = \sin(2\alpha_{\text{eff}}) \sqrt{1 - C^2}. \quad (2)$$

The angle α_{eff} coincides with α in the limit of vanishing penguin contributions. In order to constrain $\Delta\alpha \equiv \alpha - \alpha_{\text{eff}}$, techniques based on the $SU(2)$ isospin symmetry (for decays to a CP -eigenstate, such as $B^0 \rightarrow \pi^+\pi^-, \rho^+\rho^-$) or the $SU(3)$ approximate flavor symmetry (for decays to a non CP -eigenstate, such as $B^0 \rightarrow \rho^\pm\pi^\mp, a_1(1260)^\pm\pi^\mp$) have been devised, and are discussed in the remaining of this paper.

A neural network based tagging algorithm [5] is used to determine whether the B_{tag} is a B^0 or a \bar{B}^0 . Events are separated according to the particle content of the B_{tag} final state into events where there are leptons, kaons and pions, for a total of seven mutually exclusive categories. The performance of the tagging algorithm is characterized by the efficiency ϵ_{tag} in the determination of the flavor of B_{tag} and by the mistag probability ω , and depends on the tagging category. The Δt distribution of Eq. 1 is convolved with a detector resolution function, which differs for signal and background, and is parameterized as a triple Gaussian. Dilution from incorrect assignment of the flavor of B_{tag} is also taken into account:

$$\frac{dN}{d\Delta t_{meas}} = \frac{e^{-|\Delta t|/\tau}}{4\tau} \times \left\{ 1 - q_{tag} \Delta\omega - q_{tag}(1 - 2\omega) \left[C \cos(\Delta m_d \Delta t) - S \sin(\Delta m_d \Delta t) \right] \right\} \otimes R(\Delta t_{meas} - \Delta t), \quad (3)$$

where $(1 - 2\omega)$ is the dilution factor, $\Delta\omega$ is the difference in mistag probabilities $\Delta\omega \equiv \omega_{B^0} - \omega_{\bar{B}^0}$ and R is the resolution function. The parameters of the resolution function are obtained from a fit to a large sample of fully reconstructed B decays, as in [5], and are free to differ between tagging categories.

The analyses of the two-body and quasi-two-body decays described in the remaining of this paper rely on a common strategy for the suppression of the continuum $e^+e^- \rightarrow q\bar{q}$ background ($q = u, d, s, c$), which represents the most abundant source of background. Two kinematic variables, the energy substituted mass $m_{ES} = \sqrt{s/4 - p_B^2}$ and the energy difference $\Delta E = E_B - \sqrt{s}/2$, where \sqrt{s} is the e^+e^- CM energy and the four-momentum (E_B, p_B) of the B meson is defined in the CM frame, allow to discriminate correctly reconstructed B candidates (for which the distribution of m_{ES} peaks at the B -meson mass and that of ΔE peaks at zero) and fake candidates resulting from random combination of particles (for which m_{ES} follows a phase-space distribution and ΔE is approximately flat). Topological variables provide further distinction between the jet-like shape of continuum events and the more isotropic B decays, and can be combined into multivariate classifiers, such as neural network and Fisher discriminant, to enhance the discriminating power. The signal and background yields and CP asymmetries are extracted via an extended unbinned maximum-likelihood (ML) fit to the data.

3. Isospin analysis of $B \rightarrow \pi\pi$ decays

3.1. $B^0 \rightarrow \pi^+\pi^-$

In the $\pi\pi$ system the penguin pollution is greatest. The tree (T) and penguin (P) amplitudes each contribute, with different weak (ϕ) and strong (δ) phases, with comparable magnitude. Direct CP violation, which is given by $A_{CP} = 2 \sin \phi \sin \delta / (|T/P| + |P/T| + 2 \cos \phi \cos \delta)$, can, therefore, be within observational reach.

$B^0 \rightarrow \pi^+\pi^-$ decays are analyzed with the full BaBar dataset of 467 ± 5 million $B\bar{B}$ pairs [6]. A simultaneous ML fit to the $\pi^+\pi^-$, π^+K^- , $K^+\pi^-$, and K^+K^- final states is performed. $K - \pi$ separation is obtained by particle-identification (PID) observables (the Cherenkov angle Θ_C in the DIRC [7] and ionization-energy loss dE/dx in the tracking devices [8]). Additional separation between the final states under study is achieved from ΔE : since the B meson is reconstructed from two oppositely charged tracks that are both given the pion mass hypothesis, each charged K in the final state results in a ΔE displacement of about -45 MeV. We extract 1394 ± 54 signal events. From the time distribution of $B^0 \rightarrow \pi^+\pi^-$ decays a non-zero mixing-induced

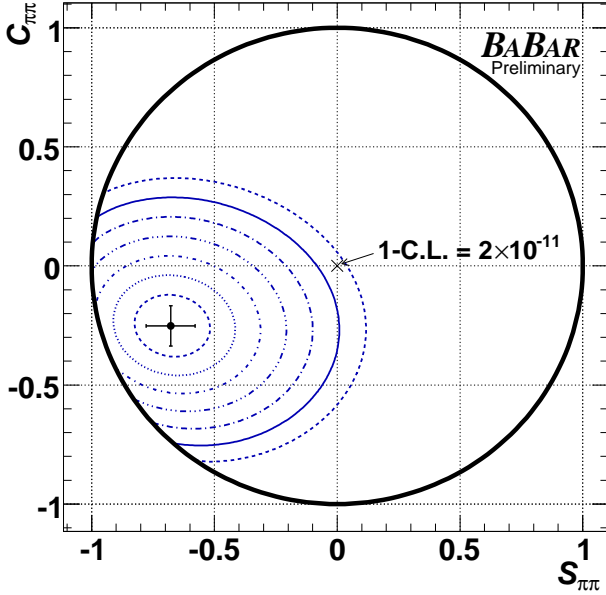


Figure 1: $S_{\pi\pi}^{+-}$ and $C_{\pi\pi}^{+-}$ in $B^0 \rightarrow \pi^+\pi^-$: the central values, errors, and confidence-level (CL) contours, calculated from the square root of the change in the value of $-2 \ln \mathcal{L}$ compared with its value at the minimum [6]. The systematic errors are included. The measured value is 6.7σ from the point of no CP violation ($S_{\pi\pi}^{+-} = 0$ and $C_{\pi\pi}^{+-} = 0$).

CP violation asymmetry $S_{\pi\pi}^{+-} = -0.68 \pm 0.10 \pm 0.03$ is observed with significance 6.3σ [6], as shown in Fig. 1. A non-zero direct CP violation asymmetry $C_{\pi\pi}^{+-} = -0.25 \pm 0.08 \pm 0.02$ is also extracted with significance 3.0σ [6].

3.2. $B^0 \rightarrow \pi^0\pi^0$

The $B^0 \rightarrow \pi^0\pi^0$ decay is formed from pairs of $\pi^0 \rightarrow \gamma\gamma$ candidates, where one of the photons can eventually be reconstructed from two tracks coming from a photon conversion $\gamma \rightarrow e^+e^-$ inside the electromagnetic calorimeter.

The yield and the flavor tag- and time-integrated CP asymmetry $A_{CP}^{00} = -C_{\pi\pi}^{00}$ are obtained from a ML fit to the kinematic variables ΔE and m_{ES} and the output of a neural network NN computed from event-shape variables, as well as the output of the B -flavor tagging algorithm. The background model accounts for correlations between NN and m_{ES} . We observe 247 ± 29 signal events (corresponding to $\mathcal{B}(B^0 \rightarrow \pi^0\pi^0) = (1.83 \pm 0.21 \pm 0.13) \times 10^{-6}$) and extracts $C_{\pi\pi}^{00} = -0.43 \pm 0.26 \pm 0.05$ [6]. Since no reliable vertex information is extracted, $S_{\pi\pi}^{00}$ can not be determined.

3.3. Isospin analysis of $B \rightarrow \pi\pi$ decays

The rates and CP asymmetries of $B^0 \rightarrow \pi^+\pi^-$ and $B^0 \rightarrow \pi^0\pi^0$ decays are combined with the results for

the $B^+ \rightarrow \pi^+\pi^0$ mode in a model-independent isospin analysis [9]. Under the isospin symmetry, $B \rightarrow \pi\pi$ amplitudes can be decomposed in isospin $I = 0$ (A_0) and $I = 2$ (A_2) amplitudes. By virtue of Bose statistics, $I = 1$ contributions are forbidden. The following relations hold [9]:

$$(1/\sqrt{2})A^{+-} = A_2 - A_0, \quad (4)$$

$$A^{00} = 2A_2 + A_0, \quad A^{+0} = 3A_2, \quad (5)$$

where A^{ij} (\bar{A}^{ij}) are the amplitudes of B (\bar{B}) decays to the $\pi^i\pi^j$ final state. This yields the complex triangle relations:

$$\frac{1}{\sqrt{2}}A^{+-} = A^{+0} - A^{00}, \quad (6)$$

$$\frac{1}{\sqrt{2}}\bar{A}^{+-} = \bar{A}^{-0} - \bar{A}^{00}. \quad (7)$$

Tree amplitudes receive contributions from both A_0 and A_2 , while gluonic penguin diagrams are pure $I = 0$ amplitudes and do not contribute to $B^+ \rightarrow \pi^+\pi^0$ amplitudes. Possible contributions from electroweak penguins (EWP), which do not obey SU(2) isospin symmetry, are assumed to be negligible and are therefore ignored. Under this assumption, $|A^{+0}| = |\bar{A}^{-0}|$ (a sizeable contribution from EWPs would result in $|A^{+0}| \neq |\bar{A}^{-0}|$ and would be signalled by an evidence of direct CP violation in $B^+ \rightarrow \pi^+\pi^0$ decays). If A^{+0} and \bar{A}^{-0} are aligned with a suitable choice of phases, the relations (6) and (7) can be represented in the complex plane by two triangles (Fig. 2), and the phase difference between A^{+-} and \bar{A}^{+-} is $2\Delta\alpha$.

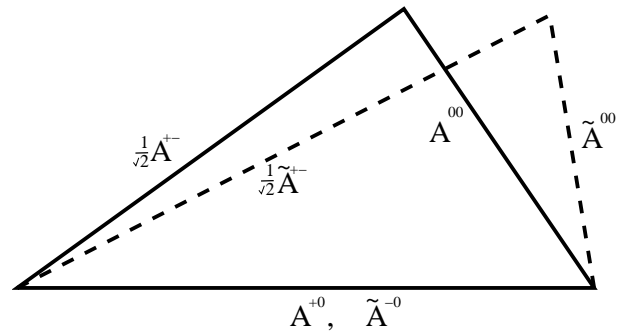


Figure 2: Triangles in the complex plane describing the isospin relations Eq. (6) and Eq. (7).

Constraints on the CKM angle α and on the penguin contribution $\Delta\alpha$ are obtained from a confidence level (CL) scan over the parameters of interest, α and $|\Delta\alpha|$. Assuming the isospin-triangle relations (6) and (7) and the expression (2), a χ^2 for the five amplitudes ($A^{+0}, A^{+-}, A^{00}, \bar{A}^{+-}, \bar{A}^{00}$) is calculated from

Table I Summary of the input to the isospin analysis of the $\pi\pi$ system [6, 10].

Mode	$\mathcal{B}(\times 10^{-6})$	C
$\pi^+\pi^-$	$5.5 \pm 0.4 \pm 0.3$	$-0.25 \pm 0.08 \pm 0.02$
$\pi^+\pi^0$	$5.02 \pm 0.46 \pm 0.29$	$(-0.03 \pm 0.08 \pm 0.01)$
$\pi^0\pi^0$	$1.83 \pm 0.21 \pm 0.13$	$-0.43 \pm 0.26 \pm 0.05$

the measurements summarized in Table I, and minimized with respect to the parameters that don't enter the scan. The $1 - CL$ values are then calculated from the probability of the minimized χ^2 .

The results of the isospin analysis are shown in Fig. 3 and Fig. 4. $\Delta\alpha$ is extracted with a four-fold ambiguity, which can be graphically represented as a flip of either triangle around A^{+0} . An additional two-fold ambiguity arises from the trigonometric relation $S_{\pi\pi}^{+-} = \sin(2\alpha_{\text{eff}})\sqrt{1 - C_{\pi\pi}^{+-2}}$. This results in a global eight-fold ambiguity in the range $[0, 180]^\circ$ on the extraction of α . A value $\Delta\alpha < 43^\circ$ at 90% CL is obtained, which dominates the uncertainty on α [6]. Considering only the solution consistent with the results of global CKM fits, α is in the range $[71, 109]^\circ$ at the 68% CL [6].

The limiting factor in the extraction of $\Delta\alpha$ is the knowledge of $|A^{00}|$ and $|\bar{A}^{00}|$, which is severely limited by the available statistics. A significant increase in statistics is therefore required in order to perform a precision measurement of α in this channel. A measurement of $S_{\pi\pi}^{00}$, which would aid resolving some ambiguities on α , can only be addressed with Super B factory luminosities [11].

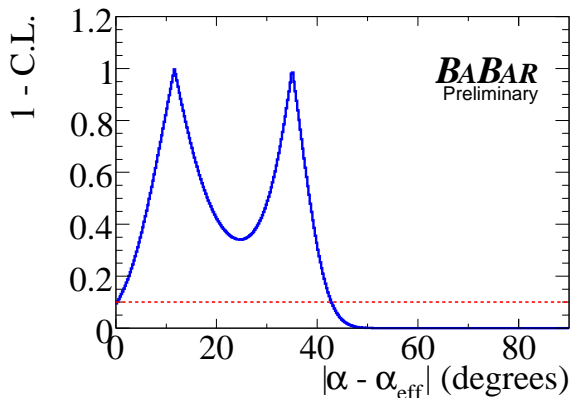


Figure 3: Projection of the $1 - CL$ scan on $\Delta\alpha$ for the $\pi\pi$ system [6].

4. Isospin analysis of $B \rightarrow \rho\rho$ decays

With respect to $B \rightarrow \pi\pi$ decays, $B \rightarrow \rho\rho$ decays have a more favourable penguin to tree amplitude ratio. Moreover, the BF for $B^0 \rightarrow \rho^+\rho^-$ decays is greater than that for $B^0 \rightarrow \pi^+\pi^-$ decays by a factor of ≈ 5 [12]. Finally, the $B^0 \rightarrow \rho^0\rho^0$ decay can be reconstructed from a final state consisting of all charged tracks, with enough efficiency to allow for a measurement of $S_{\rho\rho}^{00}$ with the present statistics [13]. Despite these many advantages with respect to the isospin analysis of $\pi\pi$ decays, the $\rho\rho$ system exhibits some potential complications.

In $B^0 \rightarrow \rho^+\rho^-$ transitions, a pseudo-scalar particle decays into two vector mesons. Three helicity states ($H = 0, \pm 1$), with different CP transformation properties, can therefore contribute to the decay [14]. The $H = 0$ state corresponds to longitudinal polarization and is CP -even, while the transverse polarization states $H = +1$ and $H = -1$ (which are superpositions of S-, P-, and D-wave amplitudes) have not a definite CP -eigenvalue. Isospin relations similar to Eq. (6) and (7) hold separately for each polarization state. The analysis of the angular distribution of $B^0 \rightarrow \rho^+\rho^-$ decays allows to determine the longitudinal polarization fraction f_L :

$$\frac{1}{\Gamma} \frac{d^2\Gamma}{d \cos \theta_1 d \cos \theta_2} \propto 4f_L \cos^2 \theta_1 \cos^2 \theta_2 + (1 - f_L) \sin^2 \theta_1 \sin^2 \theta_2, \quad (8)$$

where θ_1 (θ_2) is the angle between the daughter π^0 and the direction opposite to the B direction in the ρ^+ (ρ^-) rest frame, as shown in Fig. 5. Since experimental measurements have shown the decay to be dominated by the longitudinal, CP -even polarization, it is not necessary to separate the definite- CP contributions of the transverse polarization by means of a full angular analysis.

A second complication arises because the ρ mesons have finite width, thus allowing for the two ρ mesons

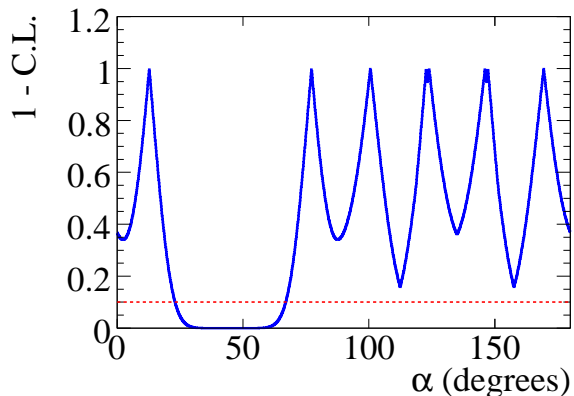


Figure 4: Projection of the $1 - CL$ scan on α for the $\pi\pi$ system [6].

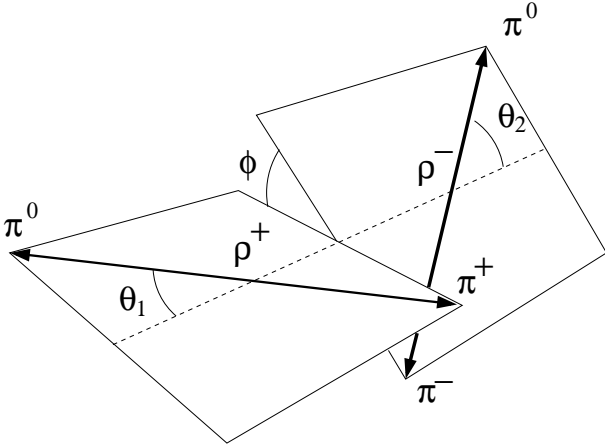


Figure 5: Definition of the θ_1 and θ_2 angles in $B \rightarrow \rho\rho$ decays [12].

in the decay to have different masses. Since the Bose-Einstein symmetry does not hold, the wave function of the $\rho\rho$ system can be anti-symmetric, and isospin $I = 1$ amplitudes are allowed, breaking the isospin relations Eq. (6) and (7) [15]. The stability of the fitted CP -violation parameters against the restriction of the $\pi\pi$ invariant mass window used to select the ρ candidates shows however that possible isospin violation effects are below the current sensitivity.

4.1. $B^+ \rightarrow \rho^+\rho^0$

The $B^+ \rightarrow \rho^+\rho^0$ decay analysis has been updated using the final BaBar dataset of 424 fb^{-1} [16], superseding the previous analysis based on 211 fb^{-1} [17]. An analysis of the angular distributions of $B^+ \rightarrow \rho^+\rho^0$ decays is performed. The signal yield and longitudinal polarization fraction is extracted via a ML fit to the kinematic quantities m_{ES} , ΔE , the output of a neural network NN based on event-shape variables, the mass of the ρ^+ and ρ^0 candidates, and the cosines of the helicity angles θ_{ρ^+} and θ_{ρ^0} , where θ_{ρ^+} (θ_{ρ^0}) is the angle between the daughter π^0 (π^-) and the direction opposite to the B direction in the ρ^+ (ρ^0) rest frame.

Improvements have been introduced on the charged particle reconstruction and on the background model, which takes into account correlations between NN , the cosine of the helicity angle, and the $\pi\pi$ invariant mass for each ρ meson in the final state. The measured BF increases from $(18.2 \pm 3.0) \times 10^{-6}$ [17] up to $(23.7 \pm 1.4 \pm 1.4) \times 10^{-6}$ [16]. The longitudinal polarization fraction is $f_L = 0.950 \pm 0.015 \pm 0.006$ [16]. The measured direct CP -violation asymmetry $A_{CP} \equiv \frac{\Gamma(B^- \rightarrow \rho^- \rho^0) - \Gamma(B^+ \rightarrow \rho^+ \rho^0)}{\Gamma(B^- \rightarrow \rho^- \rho^0) + \Gamma(B^+ \rightarrow \rho^+ \rho^0)}$ is $A_{CP} = -0.054 \pm 0.055 \pm 0.010$, which is consistent with 0. This result indicates that the contribution from EWPs is negligible, and the isospin analysis holds within an uncertainty of $1 - 2^\circ$ [18].

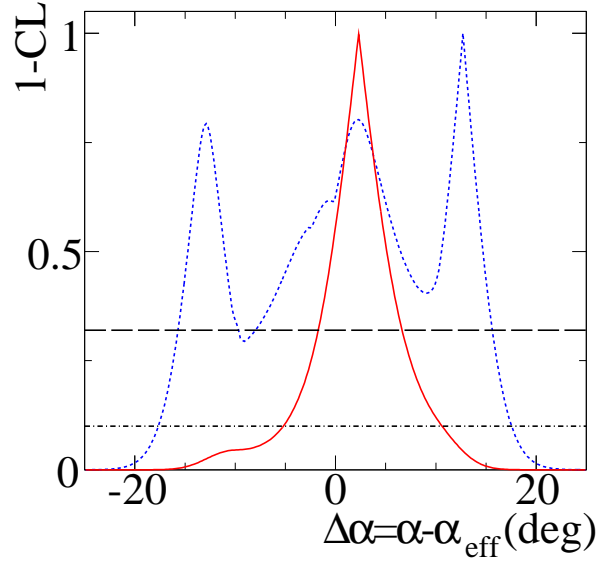


Figure 6: Projection of the $1 - CL$ scan on $\Delta\alpha$ for the $\rho\rho$ system [16].

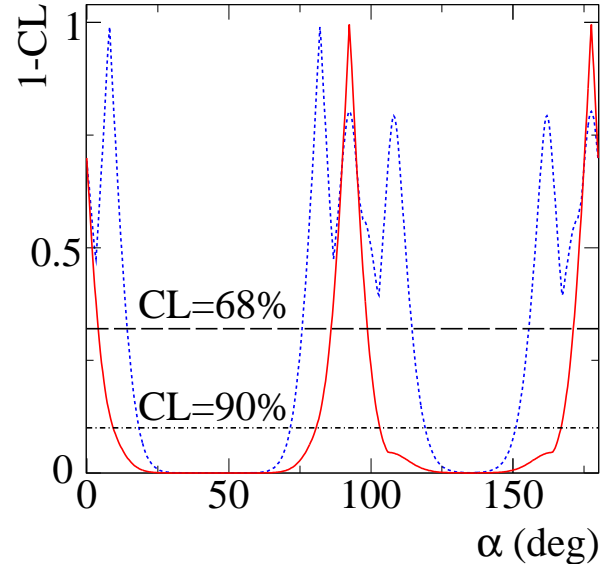


Figure 7: Projection of the $1 - CL$ scan on α for the $\rho\rho$ system [16].

The BFs, longitudinal polarization fractions, direct and mixing-induced CP violation asymmetries for $B \rightarrow \rho\rho$ decays are used as input to the isospin analysis, and are summarized in Table II. The BF's of $B^+ \rightarrow \rho^+\rho^0$ and $B^0 \rightarrow \rho^+\rho^-$ are now very similar and much higher than that for the $B^0 \rightarrow \rho^0\rho^0$ penguin transition. As a consequence, the isospin triangles do not close, *i.e.* $|A^{+-}|/\sqrt{2} + |A^{00}| < |A^{+0}|$. This results in a degeneracy of the eight-fold ambiguity on α into a four-fold ambiguity, corresponding to peaks in the vicinity of 0° , 90° (two degenerate peaks), 180° , as shown in Fig. 6 and Fig. 7. A value

Table II Summary of the input to the isospin analysis of the $\rho\rho$ system [12, 13, 16].

Mode	$\mathcal{B}(\times 10^{-6})$	f_L	\mathcal{C}	\mathcal{S}
$\rho^+\rho^-$	$25.5 \pm 2.1^{+3.6}_{-3.9}$	$0.992 \pm 0.024^{+0.026}_{-0.013}$	$0.01 \pm 0.15 \pm 0.06$	$-0.17 \pm 0.20^{+0.05}_{-0.06}$
$\rho^+\rho^0$	$23.7 \pm 1.4 \pm 1.4$	$0.950 \pm 0.042 \pm 0.006$	$(0.054 \pm 0.055 \pm 0.010)$	-
$\rho^0\rho^0$	$0.92 \pm 0.32 \pm 0.14$	$0.75^{+0.11}_{-0.14} \pm 0.04$	$0.2 \pm 0.8 \pm 0.3$	$0.3 \pm 0.7 \pm 0.2$

$-1.8^\circ < \Delta\alpha < 6.7^\circ$ at 68% CL is obtained. Considering only the solution consistent with the results of global CKM fits, $\alpha = 92.4^{+6.0}_{-6.5}$. The precision on α is now at the level of 5%.

5. $B^0 \rightarrow a_1(1260)^\pm \pi^\mp$

It is possible to extract α from B decays to final states that are not CP -eigenstates [19], such as $B^0 \rightarrow a_1(1260)^\pm \pi^\mp$ decays. The relevant amplitudes are:

$$A_+ \equiv A(B^0 \rightarrow a_1^+ \pi^-), \quad \bar{A}_+ \equiv A(\bar{B}^0 \rightarrow a_1^- \pi^+), \quad (9)$$

$$A_- \equiv A(B^0 \rightarrow a_1^- \pi^+), \quad \bar{A}_- \equiv A(\bar{B}^0 \rightarrow a_1^+ \pi^-). \quad (10)$$

The time distribution for this decay mode is given by:

$$\frac{dN a_1^\pm \pi^\mp}{d\Delta t_{meas}} = (1 \pm A_{CP}) \frac{e^{-|\Delta t|/\tau}}{4\tau} \left\{ 1 - q_{tag} \Delta\omega + q_{tag} (1 - 2\omega) \left[(S \pm \Delta S) \sin(\Delta m_d \Delta t) - (C \pm \Delta C) \cos(\Delta m_d \Delta t) \right] \right\} \otimes R(\Delta t_{meas} - \Delta t),$$

where A_{CP} is the time- and flavor-integrated charge asymmetry, and

$$S \pm \Delta S \equiv \frac{2\text{Im}(e^{-2i\beta} \bar{A}_\mp A_\pm^*)}{|A_\pm|^2 + |\bar{A}_\mp|^2}, \quad (11)$$

$$C \pm \Delta C \equiv \frac{|A_\pm|^2 - |\bar{A}_\mp|^2}{|A_\pm|^2 + |\bar{A}_\mp|^2}. \quad (12)$$

The measured CP -violation parameters for $B^0 \rightarrow a_1(1260)^\pm \pi^\mp$ decays are summarized in Table III [20].

Table III Values of the CP -violation parameters used as input to the calculation of the bounds on $|\Delta\alpha|$ [20].

A_{CP}	$-0.07 \pm 0.07 \pm 0.02$
\mathcal{S}	$0.37 \pm 0.21 \pm 0.07$
$\Delta\mathcal{S}$	$-0.14 \pm 0.21 \pm 0.06$
\mathcal{C}	$-0.10 \pm 0.15 \pm 0.09$
$\Delta\mathcal{C}$	$0.26 \pm 0.15 \pm 0.07$

In analogy to the $\pi^+\pi^-$ case, where

$$2\alpha_{\text{eff}} = \arg[e^{-2i\beta} A(\bar{B}^0 \rightarrow \pi^+\pi^-) A^*(B^0 \rightarrow \pi^+\pi^-)],$$

it is possible to define two quantities α_{eff}^+ and α_{eff}^- :

$$\alpha_{\text{eff}}^\pm \equiv \arg[e^{-2i\beta} \bar{A}_\pm A_\pm^*], \quad (13)$$

which are related by the phase $\hat{\delta} \equiv \arg[A_+ A_+^*]$ to the measurable quantities:

$$2\alpha_{\text{eff}}^\pm \pm \hat{\delta} = \arg[e^{-2i\beta} \bar{A}_\pm A_\mp^*] \quad (14)$$

$$= \arcsin \frac{S \mp \Delta S}{\sqrt{1 - (C \mp \Delta C)^2}}. \quad (15)$$

In the limit of zero penguin amplitudes, $\hat{\delta}$ coincides with the strong phase difference between the tree amplitudes contributing to $B^0 \rightarrow a_1(1260)^+ \pi^-$ and $B^0 \rightarrow a_1(1260)^- \pi^+$ decays. An effective value α_{eff} for the weak phase α is then obtained as the average $\alpha_{\text{eff}} = \frac{1}{2}(\alpha_{\text{eff}}^+ + \alpha_{\text{eff}}^-)$ with an eight-fold ambiguity [21].

It is possible to apply arguments based on the approximate SU(3) flavor symmetry to set bounds on $|\Delta\alpha|$. The following ratios of CP -averaged rates of $\Delta S = 0$ and $\Delta S = 1$ transitions are calculated, that involve the same SU(3) flavor multiplet as $a_1(1260)$ [21], such as $B^0 \rightarrow a_1(1260)^- K^+$, $B^0 \rightarrow K_{1A}^+ \pi^-$, $B^+ \rightarrow a_1(1260)^+ K^0$, and $B^+ \rightarrow K_{1A}^0 \pi^+$:

$$R_+^0 \equiv \frac{\bar{\lambda}^2 f_{a_1}^2 \bar{\mathcal{B}}(B^0 \rightarrow K_{1A}^+ \pi^-)}{f_{K_{1A}}^2 \bar{\mathcal{B}}(B^0 \rightarrow a_1^+ \pi^-)}, \quad (16)$$

$$R_+^+ \equiv \frac{\bar{\lambda}^2 f_{a_1}^2 \bar{\mathcal{B}}(B^+ \rightarrow K_{1A}^0 \pi^+)}{f_{K_{1A}}^2 \bar{\mathcal{B}}(B^+ \rightarrow a_1^+ \pi^+)}, \quad (17)$$

$$R_-^0 \equiv \frac{\bar{\lambda}^2 f_K^2 \bar{\mathcal{B}}(B^0 \rightarrow a_1^- K^+)}{f_K^2 \bar{\mathcal{B}}(B^0 \rightarrow a_1^- \pi^+)}, \quad (18)$$

$$R_-^+ \equiv \frac{\bar{\lambda}^2 f_K^2 \bar{\mathcal{B}}(B^+ \rightarrow a_1^+ K^0)}{f_K^2 \bar{\mathcal{B}}(B^+ \rightarrow a_1^+ \pi^+)}. \quad (19)$$

The bounds are effective because the penguin contribution is CKM enhanced by $1/\bar{\lambda} = |V_{cs}|/|V_{cd}|$ in $\Delta S = 1$ decays with respect to $\Delta S = 0$ modes. The following inequalities involving $(\alpha_{\text{eff}}^\pm - \alpha)$ hold:

$$\cos 2(\alpha_{\text{eff}}^\pm - \alpha) \geq \frac{1 - 2R_\pm^0}{\sqrt{1 - A_{CP}^{\pm 2}}} \quad (20)$$

$$\cos 2(\alpha_{\text{eff}}^\pm - \alpha) \geq \frac{1 - 2R_\pm^+}{\sqrt{1 - A_{CP}^{\pm 2}}}, \quad (21)$$

where A_{CP}^\pm are the direct CP asymmetries

$$A_{CP}^\pm \equiv \frac{|\bar{A}_\pm|^2 - |A_\pm|^2}{|\bar{A}_\pm|^2 + |A_\pm|^2}. \quad (22)$$

The above relations set a constraint on $(\alpha_{\text{eff}}^\pm - \alpha)$. Bounds on $|\Delta\alpha|$ are then derived from $|\Delta\alpha| \leq (|\alpha_{\text{eff}}^+ - \alpha| + |\alpha_{\text{eff}}^- - \alpha|)/2$.

The BF's of $B \rightarrow a_1(1260)\pi$ and $B \rightarrow a_1(1260)K$ decays have been measured in the last few years [20]. The measurement of the missing piece of input, the BF's of $B \rightarrow K_1(1270)\pi$ and $B \rightarrow K_1(1400)\pi$ decays, is described in the following section.

5.1. $B \rightarrow K_1(1270)\pi$, $B \rightarrow K_1(1400)\pi$

The K_{1A} meson (the SU(3) partner of the $a_1(1260)$ meson) is a nearly equal superposition of the physical states $K_1(1270)$ and $K_1(1400)$. The rates of $B \rightarrow K_{1A}\pi$ decays, which are experimental inputs to the calculation of the bounds on $|\Delta\alpha|$, must be derived from the measurement of the rates of $B \rightarrow K_1(1270)\pi$ and $B \rightarrow K_1(1400)\pi$ decays. The BF's for these processes have recently been measured by BaBar [22]. The $K_1(1270)$ and $K_1(1400)$ axial vector mesons are broad resonances with nearly equal masses. In the following, we will refer to them collectively as K_1 . The $K_1(1270)$ and $K_1(1400)$ mesons decay to the same final state $K\pi\pi$, although through different intermediate states. However, since the intermediate decays proceed almost at threshold, the available phase spaces overlap and interference effects can be sizeable. The analysis strategy relies on the reconstructed $K\pi\pi$ invariant mass spectrum in the [1.1, 1.8] GeV range to distinguish between $K_1(1270)$ and $K_1(1400)$, including interference effects in the signal model.

A two-resonance, six-channel K -matrix model is used to describe the resonant $K\pi\pi$ system for the signal [23]. The production amplitude for channel $i = \{(K^*\pi)_{S\text{-wave}}, (K^*\pi)_{D\text{-wave}}, \rho K, K_0^*\pi, f_0 K, \omega K\}$ is given by

$$F_i = e^{i\delta_i} \sum_j (\mathbf{1} - i\mathbf{K}\rho)_{ij}^{-1} \mathbf{P}_j, \quad (23)$$

where δ_i are offset phases with respect to the $(K^*\pi)_S$ channel,

$$K_{ij} = \frac{f_{ai}f_{aj}}{M_a - M} + \frac{f_{bi}f_{bj}}{M_b - M}, \quad (24)$$

and \mathbf{P} is the production vector

$$P_i = \frac{f_{pa}f_{ai}}{M_a - M} + \frac{f_{pb}f_{bi}}{M_b - M}. \quad (25)$$

The labels a and b refer to $K_1(1400)$ and $K_1(1270)$, respectively, and the indexes i and j refer to the final

states of K_1 decays. The decay constants f_{ai} , f_{bi} , and the K -matrix poles M_a and M_b are real. The elements of the diagonal phase space matrix $\rho(M)$ for the process $K_1 \rightarrow 3 + 4$, $3 \rightarrow 5 + 6$ have been approximated with the form

$$\rho = \frac{2\delta_{ij}}{M} \sqrt{\frac{2m^*m_4}{m^* + m_4}} (M - m^* - m_4 + i\Delta), \quad (26)$$

where M is the mass of K_1 , m_4 is the mass of 4, m^* is the mean mass of 3 and Δ is the half width of 3.

The parameters of \mathbf{K} and the offset phases δ_i are extracted from a fit to the data collected by the WA3 experiment [23] for the intensity of the $K\pi\pi$ channels and the relative phases. For the fit to WA3 data a background term is included in the production vector.

The decay constants for the ωK channel are fixed according to the quark model [23]. The production constants f_{pa} and f_{pb} are expressed in terms of the production parameters $\zeta = (\vartheta, \phi)$: $f_{pa} \equiv \cos\vartheta$, $f_{pb} \equiv \sin\vartheta e^{i\phi}$, where $\vartheta \in [0, \pi/2]$, $\phi \in [0, 2\pi]$.

Signal Monte Carlo (MC) samples are generated by weighting the $(K\pi\pi)\pi$ population according to the amplitude $\sum_{i \neq \omega K} \langle K\pi\pi|i \rangle F_i$, where the term $\langle K\pi\pi|i \rangle$ consists of a factor describing the angular distribution of the $K\pi\pi$ system resulting from K_1 decay, an amplitude for the resonant $\pi\pi$ and $K\pi$ systems, and isospin factors. The BF of $K_1 \rightarrow \omega K$ is accounted for as a correction to the total selection efficiency.

The BF and the production parameters ϑ, ϕ for neutral and charged B meson decays to $K_1(1270)\pi + K_1(1400)\pi$ are extracted via a ML fit to the kinematic observables m_{ES} , ΔE , a Fisher discriminant based on event-shape quantities, the $K\pi\pi$ invariant mass $m_{K\pi\pi}$ and an angular variable. Background from B decays to $K^*(1410)\pi$ and non-resonant B decays to $K^*\pi\pi$ and $\rho K\pi$ are taken into account as separate components in the fit. The dependence of the signal probability distribution in $m_{K\pi\pi}$ and selection efficiencies on the production parameters ζ is described by means of non-parametric templates $P(m_{K\pi\pi}|\vartheta, \phi)$.

Each event is classified according to the invariant masses of the $\pi^+\pi^-$ and $K^+\pi^-$ ($K_S^0\pi^+$) systems in the K_1^+ (K_1^0) decay for B^0 (B^+) candidates: events which satisfy the requirement $0.846 < m_{K\pi} < 0.946$ GeV belong to class 1 (“ K^* band”); events not included in class 1 for which $0.500 < m_{\pi\pi} < 0.800$ GeV belong to class 2 (“ ρ band”); all other events are rejected.

For the B^0 modes a likelihood scan is performed with respect to ϑ and ϕ . At each point, a simultaneous fit to the event classes $r = 1, 2$ is performed. Although for events in the “ ρ band” the signal to background ratio is worse than that for events in the “ K^* band”, MC studies have shown that including those events in the fit helps in resolving the ambiguities in the determination of the parameter ϕ . For the B^+ modes, simulations show that, due to a less favourable signal to background ratio and increased background from

B decays, the analysis is not sensitive to ϕ . A value $\phi = \pi$ is therefore assumed and the scan is performed only with respect to ϑ . At each point of the scan, a fit to “ K^* band” events only is performed.

Figure 8 shows the distribution of ΔE , m_{ES} and $m_{K\pi\pi}$ for the signal events obtained by the background-subtraction technique sPlot [24].

The experimental two-dimensional likelihood \mathcal{L} for ϑ and ϕ is convolved with a two-dimensional Gaussian that accounts for the systematic uncertainties. The resulting distributions in ϑ and ϕ are shown in Fig. 9 (the 68% and 90% probability regions are shown in dark and light shading respectively, and are defined as the regions which satisfy $\mathcal{L}(r) > \mathcal{L}_{min}$ and $\int_{\mathcal{L}(r) > \mathcal{L}_{min}} \mathcal{L}(\vartheta, \phi) d\vartheta d\phi = 68\%$ (90%).

A combined signal for B^0 decays to $K_1(1270)^+\pi^-$ and $K_1(1400)^+\pi^-$ is observed with a significance of 7.5σ , while there’s evidence for B^+ decays to $K_1(1270)^0\pi^+$ and $K_1(1400)^0\pi^+$ at 3.2σ . The measured BFs are $\mathcal{B}(B^0 \rightarrow K_1^+\pi^- + K_1^+\pi^-) = 31_{-7}^{+8} \times 10^{-6}$ and $\mathcal{B}(B^+ \rightarrow K_1^0\pi^+ + K_1^0\pi^+) = 29_{-17}^{+29} \times 10^{-6}$ ($< 82 \times 10^{-6}$ at 90% probability), including systematic uncertainties [22].

The probability distributions for the $B \rightarrow K_1(1270)\pi$, $B \rightarrow K_1(1400)\pi$, and $B \rightarrow K_{1A}\pi$ BFs are derived by setting the production parameters (f_{pa}, f_{pb}) equal to $(0, e^{i\phi} \sin \vartheta)$, $(\cos \vartheta, 0)$, and $(|f_{pA}| \cos \theta, -|f_{pA}| \sin \theta)$, respectively, where $f_{pA} = \cos \vartheta \cos \theta - e^{i\phi} \sin \vartheta \sin \theta$ and θ is the K_1 mixing angle. A value $\theta = 72^\circ$ is used [22].

Including systematic uncertainties the following values are obtained (in units of 10^{-6}): $\mathcal{B}(B^0 \rightarrow K_1(1270)^+\pi^-) = 17_{-11}^{+8}$, $\mathcal{B}(B^0 \rightarrow K_1(1400)^+\pi^-) = 17_{-9}^{+7}$, $\mathcal{B}(B^0 \rightarrow K_{1A}^+\pi^-) = 14_{-10}^{+9}$, $\mathcal{B}(B^+ \rightarrow K_1(1270)^0\pi^+) < 40$, $\mathcal{B}(B^+ \rightarrow K_1(1400)^0\pi^+) < 39$, $\mathcal{B}(B^+ \rightarrow K_{1A}^0\pi^+) < 36$, where the upper limits are evaluated at 90% probability [22].

5.2. Extraction of α

A MC technique is used to estimate a probability region for the bound on $|\Delta\alpha|$. The CP -averaged rates and CP -violation parameters participating in the estimation of the bounds are generated according to the experimental distributions; a summary of the experimental values used as input to this calculation is provided in Table IV.

For each set of generated values, the bound on $|\Delta\alpha|$ is evaluated. The limits on $|\Delta\alpha|$ are obtained by counting the fraction of bounds within a given value and the results are $|\Delta\alpha| < 11.1^\circ (13.1^\circ)$ at 68% (90%) probability [22].

The angle α is extracted with an eight-fold ambiguity in the range $[0, 180]^\circ$. The eight solutions are $\alpha = (11 \pm 7 \pm 11)^\circ$, $\alpha = (41 \pm 7 \pm 11)^\circ$, $\alpha = (49 \pm 7 \pm 11)^\circ$, $\alpha = (79 \pm 7 \pm 11)^\circ$, $\alpha = (101 \pm 7 \pm 11)^\circ$, $\alpha = (131 \pm 7 \pm 11)^\circ$, $\alpha = (139 \pm 7 \pm 11)^\circ$, $\alpha = (169 \pm 7 \pm 11)^\circ$.

Table IV Summary of the $B \rightarrow a_1(1260)\pi$ and $B \rightarrow a_1(1260)K$ branching fractions (in units of 10^{-6}) and of the form factors (in MeV) used in the calculation of α .

$\mathcal{B}(a_1^\pm \pi^\mp)$ [20]	$\mathcal{B}(a_1^- K^+)$ [20]	$\mathcal{B}(a_1^+ K^0)$ [20]	
$33.2 \pm 3.8 \pm 3.0$	$16.3 \pm 2.9 \pm 2.3$	$33.2 \pm 5.0 \pm 4.4$	
f_π [4]	f_K [4]	f_{a_1} [25]	$f_{K_{1A}}$ [26]
130.4 ± 0.2	155.5 ± 0.9	203 ± 18	207 ± 20

Assuming that the strong phase $\hat{\delta}$ is negligible [21], only two solutions are still allowed. Considering only the solution consistent with the results of global CKM fits, $\alpha = (79 \pm 7 \pm 11)^\circ$.

6. Conclusion

Recent updates of measurements related to the determination of α have been presented.

The first measurement of the branching fraction of $B \rightarrow K_1\pi$ decays, combined with the input from the analysis of the time-dependent CP -violation asymmetries in $B^0 \rightarrow a_1(1260)^\mp \pi^\pm$ decays and of the branching fractions of $B \rightarrow a_1(1260)K$ decays, allows to measure α in the $a_1(1260)\pi$ system. This novel determination of α is independent from, and consistent with, the current averages, which are based on the analysis of the $\pi\pi$, $\rho\pi$, and $\rho\rho$ systems only.

With the new update of the $B^+ \rightarrow \rho^0 \rho^+$ branching fraction and longitudinal polarization fraction measurements, the determination of α in the $\rho\rho$ system has reached the unprecedented precision of 7%, comparable with the 5.3% precision achieved in $\sin 2\beta$ measurements.

In the $\pi\pi$ system, the updated measurement of CP -violating asymmetries in $B^0 \rightarrow \pi^+\pi^-$ decays provides a 6.7σ evidence of CP violation. $B^0 \rightarrow \pi^0\pi^0$ decays branching fraction and direct CP asymmetry are input to the isospin analysis of $B \rightarrow \pi\pi$ decays that is used to constrain the effect of penguin pollution on the extraction of α .

All the measurements described in this work have been performed on the final BaBar sample. Most of them are still limited by statistics, and improvement may come from next generation, very high luminosity facilities.

Acknowledgments

I would like to thank the organizers of DPF 2009 for an interesting conference and my BaBar and PEP-II collaborators for their contributions. I’m grateful to Vincenzo Lombardo and Fernando Palombo for their support and for reviewing the manuscript.

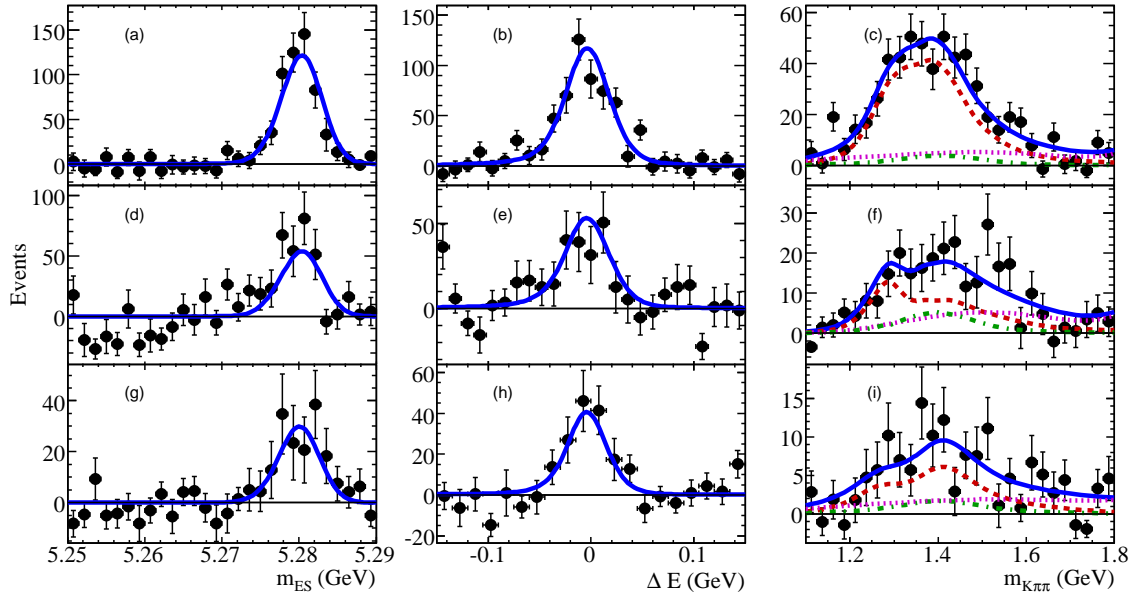


Figure 8: sPlot projections of signal onto m_{ES} (left), ΔE (center), and $m_{K\pi\pi}$ (right) for B^0 class 1 (top), B^0 class 2 (middle), and B^+ class 1 (bottom) events: the points show the sums of the signal weights obtained from on-resonance data. For m_{ES} and ΔE the solid line is the signal fit function. For $m_{K\pi\pi}$ the solid line is the sum of the fit functions of the decay modes $K_1(1270)\pi + K_1(1400)\pi$ (dashed), $K^*(1410)\pi$ (dash-dotted), and $K^*(892)\pi\pi$ (dotted), and the points are obtained without using information about resonances in the fit, *i.e.*, we use only the m_{ES} , ΔE , and \mathcal{F} variables.

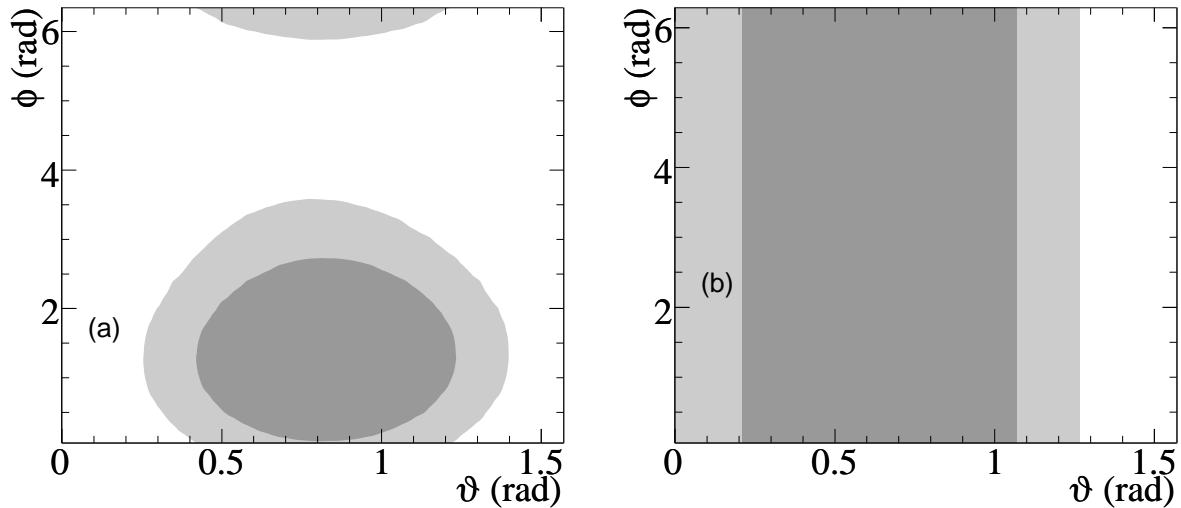


Figure 9: 68% (dark shaded zone) and 90% (light shaded zone) probability regions for ϑ and ϕ for the (a) B^0 and (b) B^+ modes.

References

- [1] N. Cabibbo, Phys. Rev. Lett. **10**, 531 (1963); M. Kobayashi and T. Maskawa, Prog. Theor. Phys. **49**, 652 (1973).
- [2] M. Bona *et al.* (UTfit Collaboration), JHEP 0603, 080 (2006).
- [3] J. Charles *et al.* (CKMFitter Group), Eur. Phys. Jour. C **41**, 1 (2005).
- [4] C. Amsler *et al.* (Particle Data Group), Phys. Lett. B **667**, 1 (2008).
- [5] B. Aubert *et al.* (BABAR Collaboration), Phys. Rev. D **66**, 032003 (2002).
- [6] B. Aubert *et al.* (BABAR Collaboration), arXiv:0807.4226 [hep-ex] (2008).
- [7] I. Adam *et al.* (BABAR-DIRC Collaboration), Nucl. Instr. Meth. A **538**, 281 (2005).
- [8] B. Aubert *et al.* (BABAR Collaboration),

- Nucl. Instr. Meth. A **479**, 1 (2002).
- [9] M. Gronau and D. London, Phys. Rev. Lett. **65**, 3381 (1990).
- [10] B. Aubert *et al.* (BABAR Collaboration), Phys. Rev. D **76**, 091102R (2007).
- [11] M. Bona *et al.*, arXiv:0709.0451 [hep-ex] (2007); S. Hashimoto *et al.*, KEK-REPORT-2004-4 (2004).
- [12] B. Aubert *et al.* (BABAR Collaboration), Phys. Rev. D **76**, 052007 (2007).
- [13] B. Aubert *et al.* (BABAR Collaboration), Phys. Rev. D **78**, 071104R (2008).
- [14] A. L. Kagan, Phys. Lett. B **601**, 151 (2004).
- [15] A. F. Falk, Z. Ligeti, Y. Nir, and H. Quinn, Phys. Rev. D **69**, 011502 (2004).
- [16] B. Aubert *et al.* (BABAR Collaboration), Phys. Rev. Lett. **102**, 141802 (2009).
- [17] B. Aubert *et al.* (BABAR Collaboration), Phys. Rev. Lett. **97**, 261801 (2006).
- [18] M. Gronau and J. Zupan, Phys. Rev. D **71**, 074017 (2005).
- [19] R. Aleksan *et al.*, Phys. Lett. B **356**, 95 (1995).
- [20] B. Aubert *et al.* (BABAR Collaboration), Phys. Rev. Lett. **97**, 051802 (2006); Phys. Rev. Lett. **98**, 181803 (2007); Phys. Rev. Lett. **100**, 051803 (2008).
- [21] M. Gronau and J. Zupan, Phys. Rev. D **73**, 057502 (2006); Phys. Rev. D **70**, 074031 (2004).
- [22] B. Aubert *et al.* (BABAR Collaboration), arXiv:0909.2171 [hep-ex] (2009).
- [23] C. Daum *et al.* (ACCMOR Collaboration), Nucl. Phys. **B187**, 1 (1981).
- [24] M. Pivk and F. R. Le Diberder, Nucl. Instr. Meth. A **555**, 356 (2005).
- [25] H.-Y. Cheng and K.-C. Yang, Phys. Rev. D **76**, 114020 (2007).
- [26] J. C. R. Bloch, Yu. L. Kalinovsky, C. D. Roberts, and S. M. Schmidt, Phys. Rev. D **60**, 111502(R) (1999).